

Anomalous magnetic flux via junction twist-angle in a triplet-superconducting transmon qubit

Sebastián Domínguez-Calderón¹ and Harley Scammell²

¹*School of Engineering and Sciences, Tecnológico de Monterrey, Monterrey 64849, México*

²*School of Mathematical and Physical Sciences, University of Technology Sydney, Ultimo, NSW 2007, Australia*

(Dated: March 13, 2024)

Superconducting transmon qubits with strong anharmonicity and insensitivity to offset charge are highly desirable for low-error implementation. In this work we propose a c-axis junction, comprising triplet superconductors, and set at a relative twist angle. Invoking spin-orbit coupling and spin polarization, which are known to occur in the material platform of choice, we examine the resulting transmon Hamiltonian. This junction allows for direct control of the single and double Cooper pair tunneling strength, and most remarkably, an anomalous magnetic flux—i.e. a phase offset equivalent to magnetic flux, yet in zero magnetic field. Having control over these three parameters—single and double pair tunneling and anomalous flux—allows for optimal design of the transmon qubit. Interestingly, in this architecture, the anomalous flux is determined by the twist angle of the junction, thereby offering a novel zero-field functionality. Our key results rely on symmetry arguments, for concreteness we demonstrate the implementation of our concept using a model of moiré graphene-based c-axis junctions.

I. INTRODUCTION

Superconducting quantum computers have undergone significant improvements and have been utilized to showcase instances of dramatic speedup compared to their classical counterparts [1]. However, a critical bottleneck in their advancement is errors [2, 3]. As the number of qubits increases, so does the number of error sources, necessitating these errors lie beneath a certain threshold; otherwise, adding more qubits becomes futile. Since true fault-tolerant quantum computation is believed to require formidable hardware resources [4, 5], the near-term goal is to dip below the error threshold. At present, superconducting quantum computers are approaching the error threshold [6], underscoring the crucial importance of further reducing errors in superconducting qubits as a primary avenue of research.

Recent advancements have pinpointed favorable transmon qubit Hamiltonians that offer tunable anharmonicity and offset charge insensitivity, thereby mitigating errors. These Hamiltonians consist of strong double Cooper pair (CP) tunneling, weak single CP tunneling, and a magnetic flux [7, 8]. One such architecture is a triple junction *d-mon* subject to magnetic flux in one junction, whereby the *d-mon* refers to a d-wave/s-wave c-axis superconducting junction. The second is a non-ideal π -SQUID, as discussed in various works [9–12], but further subjected to a magnetic flux [8].

In contrast to these works, the present study is motivated by two key questions: (i) Since magnetic fields are known inhibitors to achieving small scale devices, can we achieve the desired flux without a magnetic field? (ii) All things being equal, a single-junction qubit is more suited to small scales than a multi-junction qubit; can we design a highly tunable transmon qubit within a single junction?

The present work succeeds in designing a transmon architecture with a high tunability, within a single junction and without magnetic field. Our effective transmon maps onto two of the aforementioned recent architectures: the triple junction *d-mon* with magnetic flux [7], and the (two junction) non-ideal π -SQUID also subject to a magnetic flux [8]. Again we stress that our construction achieves this desirable qubit architecture using all-electrical control (zero magnetic field) and within a single junction. Our key innovation is the use of triplet superconductivity in the presence of spin-orbit coupling (SOC) and intrinsic magnetization. We consider a junction of spin-triplet superconductors with vectors at some non-zero angle Φ_J relative to each other on either side of the junction. Then, due to SOC, the twist angle of the junction determines Φ_J . Finally, this Φ_J acts, via a non-linear relationship, as an *anomalous* magnetic flux. This is our key finding.

Our results are of a general nature, however, for several reasons, we choose to model the key features of moiré graphene, e.g. twisted bilayer graphene, because: (i) we require triplet superconductivity, but without nodes in the order parameter, since nodes introduce decoherence [13]. A nice way to achieve this is to include an extra quantum number, in our case we choose a valley system which admits a valley quantum number. (ii) We require a valley system that can host superconductivity and moreover, triplet superconductivity. (iii) We require a superconducting valley system that can simultaneously host magnetic order. (iv) We require a system into which SOC can be induced. These criteria naturally direct us to moiré graphene. Notably, for (iv) one can proximity-induce SOC into moiré graphene via a transition metal dichalcogenide (TMD) substrate. The form of the induced SOC can be readily tuned based on the relative twist angle graphene and TMD layers [14–20].

II. BACKGROUND: TRIPLET SUPERCONDUCTIVITY IN A VALLEY SYSTEM

We provide a short summary of key details of triplet superconductivity within a valley system, subject to various particle-hole orders (e.g. spin polarization). The particular valley system considered here is modeled on moiré graphene.

First, we consider the low-energy moiré bands, and to be explicit, we consider doping with chemical potential $\mu > 0$. The partially filled moiré band is denoted $\varepsilon_{\mathbf{k}}$ and is four-fold degenerate due to spin and monolayer-valley degrees of freedom; Pauli matrices acting on these quantum numbers are denoted by s_ν and τ_ν , respectively, with $\nu = 0, x, y, z$. Moreover, we account for trigonal warping within the dispersion,

$$\varepsilon_{\mathbf{k}} = \varepsilon_{\mathbf{k}}^0(1 + \lambda\tau_z \cos 3\theta_{\mathbf{k}}) \quad (2.1)$$

where $\varepsilon_{\mathbf{k}}^0$ is rotationally symmetric, while $\cos 3\theta_{\mathbf{k}}$ reduces this symmetry to three-fold, where $\theta_{\mathbf{k}}$ is the quasi-momentum angle about a given valley. Here $\lambda < 1$ is a dimensionless parameter. See Fig. 1(a) for corresponding Fermi surfaces.

Next, our model assumes the Cooper pairs are formed from the partially-filled bands, consistent with experimental observations [21–24]. Moreover, we take the Cooper pairs to be *extended-s-wave*, i.e. being fully gapped and transforming trivially about the Fermi surface of a given valley. These orders have been discussed at various points in the literature [25–31]. Explicitly, we consider spin-triplet, valley-singlet ordering, with corresponding gap function

$$\Delta_{\mathbf{k}} = \Upsilon_{\mathbf{k}}(\mathbf{d} \cdot \mathbf{s})s_y\tau_y. \quad (2.2)$$

Here $\Upsilon_{\mathbf{k}} = \Upsilon_{\mathbf{k}}^+\delta_{\tau,+} + \Upsilon_{\mathbf{k}}^-\delta_{\tau,-}$ is composed of two complex scalar functions $\Upsilon_{\mathbf{k}}^\tau$ containing the momentum dependence of the superconducting order about the Fermi surfaces (at each valley τ); see the schematic of Fig. 1(a). Meanwhile, the three-component vector \mathbf{d} accounts for the spin triplet order parameter.

Finally, in addition to superconductivity, we include in our modeling the occurrence of different types of particle-hole orders, such as spin or valley polarization. We now provide a toy-model Hamiltonian for the partially filled moiré bands of moiré graphene with account of particle-hole orders

$$h_{\mathbf{k}} = \varepsilon_{\mathbf{k}} - \mu + M_{\mu\nu}\tau_\mu s_\nu \quad (2.3)$$

here $M_{\mu\nu}$ account for different possible particle-hole order, e.g. M_{0z} is an out-of-plane spin polarization. A schematic of these key ingredients is provided in Fig. 1(a).

III. METHODS: EFFECTIVE TRANSMON HAMILTONIAN

We model a setup of two stacked moiré graphene subsystems, separated by a thin insulating layer, and rotated to an angle Φ_J . An illustration is provided in Fig. 1(b). In this setup, we treat the systems as being two copies of moiré graphene, and crucially, the superconducting order from one system is understood to influence the other via the proximity effect. We refer to this as the moiré graphene junction — the relation to a standard Josephson junction will become apparent shortly.

In the Bogoliubov-de Gennes (BdG) framework, i.e. a mean-field Hamiltonian that captures the electronic normal state as well as the superconducting order parameters, the moiré graphene junction is modeled as,

$$H_{\mathbf{k}} = \frac{1}{2} \begin{bmatrix} h_{\mathbf{k}} & \Delta_{\mathbf{k}}^{(1)} + e^{i\varphi}\Delta_{\mathbf{k}}^{(2)} \\ \Delta_{\mathbf{k}}^{\dagger(1)} + e^{-i\varphi}\Delta_{\mathbf{k}}^{\dagger(2)} & -h_{-\mathbf{k}} \end{bmatrix}, \quad (3.1)$$

where $\Delta_{\mathbf{k}}^{(1)}$ and $\Delta_{\mathbf{k}}^{(2)}$ are the gap functions of subsystem 1 and 2, which take the form of (2.2). Note that the magnitude of $\Delta_{\mathbf{k}}^{(2)}$ will be reduced since it is proximity induced into subsystem 1, see e.g. [7] for an analogous calculation. We have made explicit the U(1) phase difference between these order parameters. We stress now that this phase difference, φ , and its canonically conjugate angular momentum, $n = -i\partial_\varphi$, will be the dynamical phase-space variables of the effective moiré graphene transmon Hamiltonian.

To arrive at the transmon Hamiltonian, we compute the free energy to quartic order in the parameter \mathbf{d} , of (2.2). Such an expansion captures both single and double tunneling processes. Explicitly, the (regularized) free energy and subsequent expansion are given by

$$\begin{aligned} \mathcal{U} &= \text{Tr} \left[\ln(\omega - H_{\mathbf{k}}) - \ln(\omega - H_{\mathbf{k}}^{(0)}) \right] \\ &\simeq -\frac{1}{2} \text{Tr} \left[\mathcal{O}_{\mathbf{k}} \mathcal{G}_{\omega, \mathbf{k}} \mathcal{O}_{\mathbf{k}} \mathcal{G}_{\omega, \mathbf{k}} \right] - \frac{1}{4} \text{Tr} \left[(\mathcal{O}_{\mathbf{k}} \mathcal{G}_{\omega, \mathbf{k}} \mathcal{O}_{\mathbf{k}} \mathcal{G}_{\omega, \mathbf{k}})^2 \right] \\ &\simeq a_1 \cos \varphi + b_1 \sin \varphi + a_2 \cos 2\varphi + b_2 \sin 2\varphi \end{aligned} \quad (3.2)$$

here $H_{\mathbf{k}}^{(0)} \equiv H_{\mathbf{k}}|_{\Delta_{\mathbf{k}}^{(i)} \rightarrow 0}$; $\mathcal{G}_{\omega, \mathbf{k}} = G_{\omega, \mathbf{k}}(\eta_0 + \eta_z)/2 - G_{-\omega, -\mathbf{k}}(\eta_0 - \eta_z)/2$ and $G_{\omega, \mathbf{k}} = [i\omega - h_{\mathbf{k}}]^{-1}$; and $\mathcal{O}_{\mathbf{k}} = \eta_+ (\Delta_{\mathbf{k}}^{(1)} + e^{i\varphi}\Delta_{\mathbf{k}}^{(2)}) + \eta_- (\Delta_{\mathbf{k}}^{\dagger(1)} + e^{-i\varphi}\Delta_{\mathbf{k}}^{\dagger(2)})$, with η_μ Pauli-matrices accounting for the Nambu space of the BdG Hamiltonian (3.1). The approximations in passing from the first-to-second and second-to-third lines involves ignoring higher-order tunneling processes, i.e. $\cos n\varphi$ for $n > 2$, and ignoring an irrelevant φ -independent offset.

Meanwhile, the charging energy of the junction takes the standard form,

$$\mathcal{K} = 4E_C(n - n_g)^2, \quad (3.3)$$

with $n = -i\partial_\varphi$ and n_g an offset *gate charge*. Together, the moiré graphene transmon Hamiltonian is $\mathcal{H} = \mathcal{K} + \mathcal{U}$.

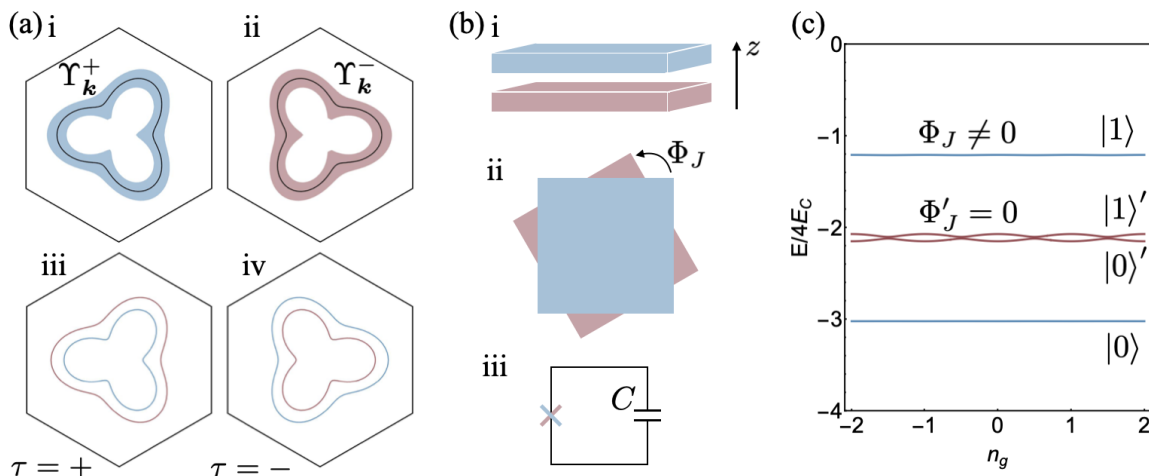


FIG. 1: Model details: (a)i&ii Fermi surfaces of $\varepsilon_{\tau\mathbf{k}}^0$ for $\tau = \pm$; gap function $\Upsilon_{\mathbf{k}}^{\tau}$ is superimposed as the shaded region. (a)iii&iv Fermi surfaces with account of spin-valley locked polarization $\varepsilon_{\tau\mathbf{k}} = \varepsilon_{\tau\mathbf{k}} + M_{zz}\tau_z s_z$, blue and red correspond to the two spin species. (b)i Schematic of the junction and (b)ii top view of the twisted junction, with twist angle Φ_J . (b)iii Shows the corresponding circuit. (c) Qubit subspace of the transmon spectrum—red eigenvalues $\{|0'\rangle, |1'\rangle\}$ corresponds to zero twist angle $\Phi_J' = 0$ (denoted with a prime for clarity), blue eigenvalues $\{|0\rangle, |1\rangle\}$ corresponds to a non-zero twist angle, $\Phi_J \neq 0$.

Truncating at double CP tunnelling, working in units of $4E_C = 1$, and choosing a simpler gauge than (3.2),

$$\mathcal{H} = (n - n_g)^2 + \alpha_1 \cos(\varphi + \Phi) + \alpha_2 \cos 2\varphi. \quad (3.4)$$

The parameters $\{\alpha_1, \alpha_2, \Phi\}$ control the anharmonicity and charge offset insensitivity (band flatness) of the qubit subspace. For more details of a specific metric, see [7]. An ideal regime corresponds to $\alpha_2 \gg \alpha_1 > 1$ with $\Phi \sim \pi/2$ — a demonstration is provided in Fig. 1(c), which compares the different qubit subspaces formed taking $\{\alpha_1, \alpha_2\} = \{20, 2\}$ and with $\Phi = \pi/2$ or 0. Dramatic improvement, with respect to band flatness (and not shown, also the anharmonicity) can be seen for $\Phi = \pi/2$ (non-zero flux). The takeaway message is that, the better the control of $\{\alpha_1, \alpha_2, \Phi\}$, the better one can design a transmon qubit. Hence, the objective of the present work is to find setups that allow control of $\{\alpha_1, \alpha_2, \Phi\}$, under the additional constraint of wanting only a single junction and zero magnetic flux. This is to be contrasted with previous proposals, which include the triple junction *d-mon* subject to magnetic flux [7] and the non-ideal π -SQUID: a superconducting loop formed by two π -periodic circuit elements, also subject to an external magnetic flux [8].

IV. RESULTS: TWISTED TRIPLET-TRIPLET JUNCTION

As our specific setup, we consider the triplet-triplet junction, i.e. with triplet vectors $\mathbf{d}^{(1)}$ and $\mathbf{d}^{(2)}$, and further impose an easy axis spin-orbit coupling, via a TMD substrate layer, see e.g. [31] for detailed discussion. The purpose is to reduce the $SO(3)$ spin-rotational symmetry

of the $\mathbf{d}^{(1,2)}$, and couple it to a given spatial (crystal) axis, i.e. $\mathbf{d}^{(1)} = d_0(1, 0, 0)$ in subsystem 1. Next, spatially rotating subsystem 2 to an angle Φ_J relative to subsystem 1, implies that $\mathbf{d}^{(2)} = d_0(\cos \Phi_J, \sin \Phi_J, 0)$; the triplet angle follows the spatial twist angle, thanks to SOC. The total gap function entering the BdG Hamiltonian (3.1) is then

$$\Delta_{\mathbf{k}}^{(1)} + e^{i\varphi} \Delta_{\mathbf{k}}^{(2)} = \Upsilon_{\mathbf{k}}(\mathbf{d}^{(1)} + e^{i\varphi} \mathbf{d}^{(2)}) \cdot \mathbf{s}(s_y \tau_y). \quad (4.1)$$

In what follows, we denote $\mathbf{d} \equiv \mathbf{d}^{(1)} + e^{i\varphi} \mathbf{d}^{(2)}$.

Finally, allowing for spin polarization — denoted $\mathbf{M} = M_z z$ and taken to be along z , i.e. appearing in (2.3) as $M_z s_z$ — the free energy expansion then permits the terms,

$$\begin{aligned} \delta\mathcal{U}_1 &\sim i\mathbf{M} \cdot (\mathbf{d}^* \times \mathbf{d}) = g_1 M_z \sin \Phi_J \sin \varphi, \\ \delta\mathcal{U}_2 &\sim i\mathbf{M} \cdot (\mathbf{d}^* \times \mathbf{d})(\mathbf{d}^* \cdot \mathbf{d}) = g_2 M_z \sin 2\Phi_J \sin 2\varphi. \end{aligned} \quad (4.2)$$

Here $g_{1,2}$ are dimensionless parameters, that can be obtained via direct computation of (3.2). The $\sin \varphi$ and $\sin 2\varphi$ contributions to the transmon potential is our key observation. Their existence relies on the vector product $(\mathbf{d}^* \times \mathbf{d}) \neq \mathbf{0}$, i.e. *non-unitary* superconductivity [32], as well as the vector \mathbf{M} associated here with spin polarization.

Armed with the above setup, and upon expanding to first-order in M_z , we arrive at the parameters of the potential (3.2) (i.e. before re-gauging to (3.4)),

$$\begin{aligned} a_1 &\sim a_1^0 \cos \Phi_J, & b_1 &\sim g_1 M_z \sin \Phi_J, \\ a_2 &\sim a_2^0 \cos 2\Phi_J, & b_2 &\sim g_2 M_z \sin 2\Phi_J. \end{aligned} \quad (4.3)$$

Here a_1^0, a_2^0 are independent of M_z to order $O(M_z^2)$. Upon re-gauging, we arrive at the transmon Hamiltonian (3.4),

with parameters

$$\alpha_1 = \sqrt{a_1^2 + b_1^2}, \quad \alpha_2 = \sqrt{a_2^2 + b_2^2}, \quad (4.4)$$

$$\Phi = \arctan\left(\frac{g_1 M_z}{a_1^0} \tan \Phi_J\right) - \frac{1}{2} \arctan\left(\frac{g_2 M_z}{a_2^0} \tan 2\Phi_J\right).$$

This constitutes the title claim: that the junction twist angle, Φ_J , generates the anomalous magnetic flux Φ , via a nonlinear relationship (4.4).

V. DISCUSSION

We examined *c*-axis tunnel junctions built from triplet superconductors. Our objective was to demonstrate that such junctions are useful for creating highly optimal transmon qubits, based on the criteria of anharmonicity and offset charge insensitivity. Leaning on two recent analyses [7, 8], we distilled the problem statement down to: how can we arrange the triplet superconductors, so as to have control over the three relevant parameters in the transmon Hamiltonian, $\{\alpha_1, \alpha_2, \Phi\}$. In our work, these parameters are understood to control, respectively, single and double CP tunneling and an anomalous (zero-field) magnetic flux that acts solely on the single tunneling processes.

To achieve our goal, we found that a spin-triplet junction, with rotated triplet vectors on either side, and in the presence of spin polarization, gave us the desired Hamiltonian. The ability to rotate the spin vector became tied to the ability to rotate the junction, thanks to spin-orbit coupling.

All of these ingredients: triplet superconductivity, spin polarization, spin-orbit interaction and a valley degree of freedom, are features of moiré graphene (with a TMD substrate), which prompted our searches in the first instance. Moreover, taking moiré graphene as the qubit platform also gives us hope that the present work will inspire near-term experimental tests, given the ongoing research activity into moiré graphene. Aside from moiré graphene, we note that triplet superconductivity in a valley system has been modeled via modulated gating of a two-dimensional electron (or hole) gas [33–35], which can also be designed to induce spin orbit coupling [36, 37]. This represents another possible avenue.

Finally, we contrast with recent works [38–40], which have achieved gate-defined Josephson junctions within moiré graphene (see also recent theory [41]); such junctions are in-plane, whereas we consider the out-of-plane (*c*-axis) junction. We leave it for future work to explore the ideas presented here within a gate defined, in-plane junction.

ACKNOWLEDGEMENTS

We thank Julian Ingham for critical feedback on the manuscript.

-
- [1] F. Arute and et al, “Quantum supremacy using a programmable superconducting processor,” *Nature* **574**, 505 (2019).
 - [2] M. Kjaergaard, M. E. Schwartz, J. Braumüller, P. Krantz, J. I.-J. Wang, S. Gustavsson, and W. D. Oliver, “Superconducting qubits: Current state of play,” *Annual Review of Condensed Matter Physics* **11**, 369 (2020), <https://doi.org/10.1146/annurev-conmatphys-031119-050605>.
 - [3] A. Gyenis, A. Di Paolo, J. Koch, A. Blais, A. A. Houck, and D. I. Schuster, “Moving beyond the transmon: Noise-protected superconducting quantum circuits,” *PRX Quantum* **2**, 030101 (2021).
 - [4] A. G. Fowler, M. Mariantoni, J. M. Martinis, and A. N. Cleland, “Surface codes: Towards practical large-scale quantum computation,” *Phys. Rev. A* **86**, 032324 (2012).
 - [5] M. Reiher, N. Wiebe, K. M. Svore, D. Wecker, and M. Troyer, “Elucidating reaction mechanisms on quantum computers,” *Proceedings of the National Academy of Sciences* **114**, 7555 (2017), <https://www.pnas.org/doi/pdf/10.1073/pnas.1619152114>.
 - [6] R. Acharya and et al, “Suppressing quantum errors by scaling a surface code logical qubit,” *Nature* **614**, 676 (2023).
 - [7] H. Patel, V. Pathak, O. Can, A. C. Potter, and M. Franz, “*d*-mon: A transmon with strong anharmonicity based on planar *c*-axis tunneling junction between *d*-wave and *s*-wave superconductors,” *Phys. Rev. Lett.* **132**, 017002 (2024).
 - [8] J. W. Staples, T. B. Smith, and A. C. Doherty, “Universal flux-based control of a π -squid,” (2024), [arXiv:2312.04321 \[quant-ph\]](https://arxiv.org/abs/2312.04321).
 - [9] A. Kitaev, “Protected qubit based on a superconducting current mirror,” (2006), [arXiv:cond-mat/0609441 \[cond-mat.mes-hall\]](https://arxiv.org/abs/cond-mat/0609441).
 - [10] A. D. Paolo, A. L. Grimsmo, P. Groszkowski, J. Koch, and A. Blais, “Control and coherence time enhancement of the $0-\pi$ qubit,” *New Journal of Physics* **21**, 043002 (2019).
 - [11] C. Ciaccia, R. Haller, A. C. C. Drachmann, T. Lindemann, M. J. Manfra, C. Schrade, and C. Schönberger, “Charge-4e supercurrent in a two-dimensional inas-al superconductor-semiconductor heterostructure,” *Communications Physics* **7**, 41 (2024).
 - [12] M. Valentini, O. Sagi, L. Baghumyan, T. de Gijzel, J. Jung, S. Calcaterra, A. Ballabio, J. Aguilera Servin, K. Aggarwal, M. Janik, T. Adletzberger, R. Seoane Souto, M. Leijnse, J. Danon, C. Schrade,

- E. Bakkers, D. Christina, G. Isella, and G. Katsaros, “Parity-conserving cooper-pair transport and ideal superconducting diode in planar germanium,” *Nature Communications* **15**, 169 (2024).
- [13] Y. V. Fominov, A. A. Golubov, and M. Y. Kupriyanov, “Decoherence due to nodal quasiparticles in d-wave qubits,” *Journal of Experimental and Theoretical Physics Letters* **77**, 587 (2003).
- [14] T. Naimier, K. Zollner, M. Gmitra, and J. Fabian, “Twist-angle dependent proximity induced spin-orbit coupling in graphene/transition metal dichalcogenide heterostructures,” *Phys. Rev. B* **104**, 195156 (2021).
- [15] Y. Li and M. Koshino, “Twist-angle dependence of the proximity spin-orbit coupling in graphene on transition-metal dichalcogenides,” *Phys. Rev. B* **99**, 075438 (2019).
- [16] A. David, P. Rakyta, A. Kormányos, and G. Burkard, “Induced spin-orbit coupling in twisted graphene–transition metal dichalcogenide heterobilayers: Twistronics meets spintronics,” *Phys. Rev. B* **100**, 085412 (2019).
- [17] S. Lee, D. J. P. de Sousa, Y.-K. Kwon, F. de Juan, Z. Chi, F. Casanova, and T. Low, “Charge-to-spin conversion in twisted graphene/wse₂ heterostructures,” *Phys. Rev. B* **106**, 165420 (2022).
- [18] C. G. Péterfalvi, A. David, P. Rakyta, G. Burkard, and A. Kormányos, “Quantum interference tuning of spin-orbit coupling in twisted van der waals trilayers,” *Phys. Rev. Research* **4**, L022049 (2022).
- [19] K. Zollner and J. Fabian, “Bilayer graphene encapsulated within monolayers of WS₂ or Cr₂Ge₂Te₆: Tunable proximity spin-orbit or exchange coupling,” *Phys. Rev. B* **104**, 075126 (2021).
- [20] K. Zollner, M. Gmitra, and J. Fabian, “Proximity spin-orbit and exchange coupling in aba and abc trilayer graphene van der waals heterostructures,” *Phys. Rev. B* **105**, 115126 (2022).
- [21] J. M. Park, Y. Cao, K. Watanabe, T. Taniguchi, and P. Jarillo-Herrero, “Tunable strongly coupled superconductivity in magic-angle twisted trilayer graphene,” *Nature* **590**, 249 (2021).
- [22] Z. Hao, A. M. Zimmerman, P. Ledwith, E. Khalaf, D. H. Najafabadi, K. Watanabe, T. Taniguchi, A. Vishwanath, and P. Kim, “Electric field-tunable superconductivity in alternating-twist magic-angle trilayer graphene,” *Science* **371**, 1133 (2021).
- [23] J.-X. Lin, P. Siriviboon, H. D. Scammell, S. Liu, D. Rhodes, K. Watanabe, T. Taniguchi, J. Hone, M. S. Scheurer, and J. I. A. Li, “Zero-field superconducting diode effect in small-twist-angle trilayer graphene,” *Nature Physics* (2022).
- [24] P. Siriviboon, J.-X. Lin, X. Liu, H. D. Scammell, S. Liu, D. Rhodes, K. Watanabe, T. Taniguchi, J. Hone, M. S. Scheurer, and J. I. A. Li, “A new flavor of correlation and superconductivity in small twist-angle trilayer graphene,” arXiv e-prints (2021), arXiv:2112.07127 [cond-mat.mes-hall].
- [25] C. Xu and L. Balents, “Topological superconductivity in twisted multilayer graphene,” *Phys. Rev. Lett.* **121**, 087001 (2018).
- [26] Y.-Z. You and A. Vishwanath, “Superconductivity from valley fluctuations and approximate so(4) symmetry in a weak coupling theory of twisted bilayer graphene,” *npj Quantum Materials* **4**, 16 (2019).
- [27] M. S. Scheurer and R. Samajdar, “Pairing in graphene-based moiré superlattices,” *Phys. Rev. Research* **2**, 033062 (2020).
- [28] E. Lake, A. S. Patri, and T. Senthil, “Pairing symmetry of twisted bilayer graphene: A phenomenological synthesis,” *Phys. Rev. B* **106**, 104506 (2022).
- [29] H. D. Scammell, J. I. A. Li, and M. S. Scheurer, “Theory of zero-field superconducting diode effect in twisted trilayer graphene,” *2D Mater.* **9**, 025027 (2022).
- [30] H. D. Scammell and M. S. Scheurer, “Tunable superconductivity and möbius fermi surfaces in an inversion-symmetric twisted van der waals heterostructure,” *Phys. Rev. Lett.* **130**, 066001 (2023).
- [31] H. D. Scammell and M. S. Scheurer, “Displacement field tunable superconductivity in an inversion-symmetric twisted van der waals heterostructure,” *Phys. Rev. B* **109**, 035159 (2024).
- [32] M. Sigrist and K. Ueda, “Phenomenological theory of unconventional superconductivity,” *Rev. Mod. Phys.* **63**, 239 (1991).
- [33] T. Li, J. Ingham, and H. D. Scammell, “Artificial graphene: Unconventional superconductivity in a honeycomb superlattice,” *Phys. Rev. Res.* **2**, 043155 (2020).
- [34] T. Li, M. Geier, J. Ingham, and H. Scammell, “Higher-order topological superconductivity from repulsive interactions in kagome and honeycomb systems,” *2D Materials* (2021).
- [35] H. D. Scammell, J. Ingham, M. Geier, and T. Li, “Intrinsic first- and higher-order topological superconductivity in a doped topological insulator,” *Phys. Rev. B* **105**, 195149 (2022).
- [36] O. P. Sushkov and A. H. Castro Neto, “Topological insulating states in laterally patterned ordinary semiconductors,” *Phys. Rev. Lett.* **110**, 186601 (2013).
- [37] H. D. Scammell and O. P. Sushkov, “Tuning the topological insulator states of artificial graphene,” *Phys. Rev. B* **99**, 085419 (2019).
- [38] J. Díez-Mérida, A. Díez-Carlón, S. Y. Yang, Y.-M. Xie, X.-J. Gao, J. Senior, K. Watanabe, T. Taniguchi, X. Lu, A. P. Higginbotham, K. T. Law, and D. K. Efetov, “Symmetry-broken josephson junctions and superconducting diodes in magic-angle twisted bilayer graphene,” *Nature Communications* **14**, 2396 (2023).
- [39] F. K. de Vries, E. Portolés, G. Zheng, T. Taniguchi, K. Watanabe, T. Ihn, K. Ensslin, and P. Rickhaus, “Gate-defined josephson junctions in magic-angle twisted bilayer graphene,” *Nature Nanotechnology* **16**, 760 (2021).
- [40] D. Rodan-Legrain, Y. Cao, J. M. Park, S. C. de la Barrera, M. T. Randeria, K. Watanabe, T. Taniguchi, and P. Jarillo-Herrero, “Highly tunable junctions and non-local josephson effect in magic-angle graphene tunnelling devices,” *Nature Nanotechnology* **16**, 769 (2021).
- [41] Y.-M. Xie, D. K. Efetov, and K. T. Law, “ φ_0 -josephson junction in twisted bilayer graphene induced by a valley-polarized state,” *Phys. Rev. Res.* **5**, 023029 (2023).